

# Electronic excitations in parabolically confined electron systems

Achim Wixforth

*Sektion Physik, Ludwig-Maximilians-Universität München, Geschwister Scholl Platz 1, D-80539 München, Germany*

## Abstract

The dynamic response of electron systems confined in a one-dimensional parabolic potential is investigated experimentally. Such structures are realized in so-called parabolic quantum wells where the parabolic confining potential is achieved by a proper grading of the barriers of a AlGaAs/GaAs quantum well. We present some of our recent studies on both intra- and interband fundamental excitations of such systems like cyclotron resonance, intersubband resonance, plasmon modes and photoluminescence excitations using various experimental techniques and geometries. Detailed studies of the electronic excitations in parabolic wells with intentionally induced deviations from ideal parabolicity allow for a better understanding of the effect of non-parabolic terms in the confining potential also for lateral nanostructures. Due to the simplicity of the confining potentials most of our experimental results can be explained in simple straightforward and transparent ways that also apply to recent investigations of lateral nanostructures and thus may serve for a better understanding also of this rapidly developing field.

## 1. Introduction

The interaction between electron systems in semiconductor quantum well structures and optical fields has been studied intensively during the last two decades [1]. These studies include intersubband absorption, cyclotron resonance in high magnetic fields as well as plasmon emission and absorption. The collective excitation spectrum of an electronic system contains valuable information as it is one of its most fundamental properties. For quasi-two-dimensional electron systems (Q2DES, quantum films) as realized in space charge layers in semiconductors the study of plasmon (intrasubband) excitations as well as intersubband transitions have proven invaluable in the characterization and understanding of these systems [2]. More recently [3], the collective excita-

tions in quasi-one-dimensional (Q1DES, quantum wires) [4,5] and quasi-zero-dimensional electron systems [6] (Q0DES, quantum dots) have also attracted very much attention. This is because in the last few years the realization of lateral nanostructures has become possible, which yielded a rapidly growing field of interest in semiconductor physics. On the other hand, tremendous improvements of semiconductor growth techniques like molecular beam epitaxy (MBE) nowadays offer the possibility to engineer practically every desired kind of bandstructure for semiconductor structures.

A very attractive application of those advanced growth methods are so-called parabolic quantum wells (PQW). Originally invented to represent an attempt towards the theoretical construct of *jellium*, it turned out that there is a striking similar-

ity of many of their properties to the ones of a Q1DES or even a Q0DES. Many experimental results obtained in such nanostructures have in the recent past also been successfully described in a parabolic approximation [3]. For this reason, throughout this report, I shall point out the similarities and the applicability of our experimental and theoretical results to the case of lateral nanostructures and give representative examples.

## 2. Electron systems in parabolic quantum wells

PQWs are grown by computer-controlled molecular beam epitaxy (MBE). The parabolic profiles of both the conduction as well as the valence bands are obtained by properly grading the aluminum content of the ternary  $\text{Al}_x\text{Ga}_{1-x}\text{As}$  alloy. In the range  $0 \leq x \leq 0.3$  its band gap varies nearly linearly with Al mole fraction, such that a controlled variation of  $x$  directly leads to the desired structure. The basic idea of these structures is thus to create a conduction band profile  $E_C(z)$  in the growth direction such that it mimics the parabolic potential of a uniformly distributed slab of positive charge  $n^+$ . Once this structure is remotely doped, the donors release electrons into the well which in turn will screen the man-made parabolic potential and form a wide and nearly homogeneous electron layer. An undoped spacer

between the dopants and the well reduces ionized impurity scattering and thus enhances the electron mobility in the well, as is the case for conventional heterostructures. The fictitious charge  $n^+$  is related to the curvature of the grown PQW by Poisson's equation:

$$n^+ = \frac{\epsilon\epsilon_0}{e^2} \frac{\partial^2 E_C}{\partial z^2} = \frac{8\epsilon\epsilon_0\Delta}{e^2 W^2}. \quad (1)$$

Here,  $\epsilon$  denotes the dielectric constant of  $\text{Al}_x\text{Ga}_{1-x}\text{As}$ ,  $\Delta$  is the energy height of the parabola from its bottom to the edges,  $e$  the electronic charge, and  $W$  the width of the grown PQW. Thus  $n^+$  can be varied over a wide range by proper control of the growth process. Typical curvatures of our samples correspond to  $n^+$  of a few times  $10^{16} \text{ cm}^{-3}$ . Due to the similarity to a real existing positive space charge, this concept has been referred to as "quasi-doping".

In Fig. 1 we depict the basic results as obtained from a self-consistent calculation of the resulting subband structure and carrier distribution in such a PQW. Since in our experiments we are able to vary the carrier density in the well by application of a gate bias between a semitransparent electrode on top of the sample and the electron system, we plot the above quantities as a function of  $V_g$ . Typical sheet carrier densities in our samples lie in the range of a few times  $10^{11} \text{ cm}^{-2}$ . Usually, up to four subbands are occupied

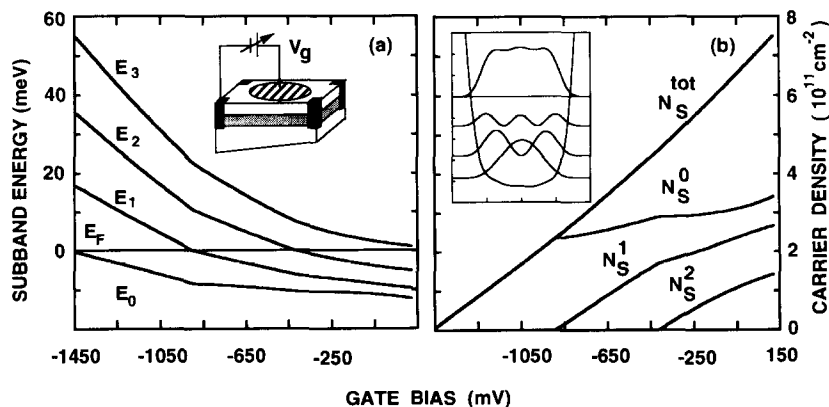


Fig. 1. (a) Self-consistent subband spacing of a wide PQW as a function of the applied gate bias  $V_g$ . The inset depicts a typical sample geometry used in our experiments. (b) Distribution of the carriers in a PQW as a function of gate bias. Decreasing gate voltage tends to deplete the well by depopulating the electrical subbands. The inset depicts the wavefunctions and the total carrier distribution in the well together with the self-consistent Hartree potential at  $V_g = 0 \text{ V}$ .

at  $V_g = 0$  V, and the resulting total carrier distribution is essentially flat over the region of the well. The self-consistent potential in this case also exhibits a flat bottom as expected for a quasi-three-dimensional electron system. Decreasing gate bias depletes the well and simultaneously increases the self-consistent subband spacing as indicated in Fig. 1a. At the same time the electrical subbands become depopulated at specific gate voltages. The slab of mobile carriers narrows thus changing its dimension from quasi 3D towards quasi 2D behavior.

### 3. Far-infrared spectroscopy

Shortly after the first successful realization of remotely doped PQWs, some initial experiments [7,8] stimulated a lot of further experimental as well as theoretical work on this subject. Subsequently, both (magneto-)transport [9,10] as well as FIR investigations [11] uncovered a large amount of new and interesting results which shed some light onto the understanding of many fundamental properties of low-dimensional electron systems.

The most interesting by-product of the initial experimental investigations of the far-infrared (FIR) response of a PQW was the formulation of the generalized Kohn theorem [12]: It states that in a purely parabolically confined electron system long-wavelength radiation only couples to the center of mass (CM) coordinates and its motion. The reason is the decoupling of these modes of the interacting electron gas from its internal modes. Relative coordinates, and thus particularly electron–electron interactions, in such systems do not affect the resonance frequency of the observed transitions. FIR experiments on a PQW thus only allow access to a single well-defined frequency  $\omega_0$  which is related to the CM motion of the whole electron system and is solely determined by the curvature of the external confining potential. For the case of a PQW this resonance frequency can be determined by the growth of the PQW alone, namely

$$\hbar\omega_0 = \left( \hbar^2 \frac{8\Delta}{W^2 m^*} \right)^{1/2}. \quad (2)$$

This mode is of inter-subband type and represents a sloshing of the electron system as a whole in the external parabolic potential. A very power-

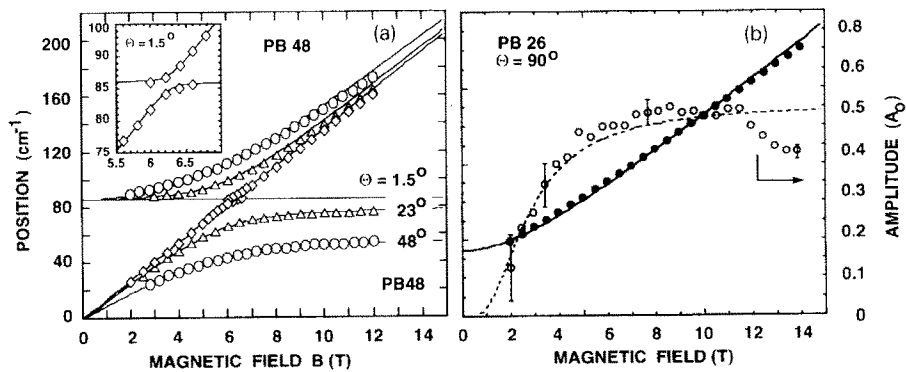


Fig. 2. (a) Experimentally obtained resonance positions for three different tilted field experiments as a function of the total magnetic field strength  $B$ . With increasing tilt angle the mode anticrossing becomes more pronounced. The solid lines are the result of a calculation according to Eq. (3) using no fit parameters for all three measurements. (b) The same experiment with the magnetic field in the plane of the PQW. This leads to a complete hybridization of the CR and the sloshing mode of the PQW. Filled symbols and the solid line represent the extracted and calculated resonance positions, open symbols and the dashed line depict the amplitude of the line as extracted from our experiment together with the theoretical one. The origin of the discrepancies between the oscillator strength as obtained experimentally and theoretically is not known to date.

ful method to investigate this sloshing mode, working well in PQWs, is the use of a tilted magnetic field which couples the in-plane motion of the mobile carriers to the vertical one. This leads to a strong interaction between the cyclotron resonance (CR)  $\omega_c = eB/m^*$  and the sloshing mode represented by  $\omega_0$ , manifested in an anti-crossing around  $\omega_c = \omega_0$ . The result is a splitting of the CR into two lines,  $\omega_+$  and  $\omega_-$ , which are given by the simple analytic expression

$$\omega_{\pm} = \sqrt{\frac{1}{2}(\omega_c^2 + \omega_0^2) \pm \frac{1}{2}\sqrt{\omega_c^4 + \omega_0^4 + 2\omega_0^2(\omega_{c,x}^2 - \omega_{c,z}^2)}}. \quad (3)$$

Here,  $\omega_{c,x} = \omega_c \sin \theta$  and  $\omega_{c,z} = \omega_c \cos \theta$  denote the projections of the CR onto the magnetic field components parallel and perpendicular to the growth direction.  $B$  is tilted by an angle  $\theta$  with respect to the sample surface. For the extreme case of a totally in-plane field, Eq. (3) converts to  $\omega_{\pm}^2 = \omega_c^2 + \omega_0^2$  representing the plasma-shifted CR, a hybrid mode between electrical and magnetic confinement. Typical experimental results are given in Fig. 2. Here, we plot the extracted resonance positions of tilted or in-plane field transmission experiments as a function of the total magnetic field. In (a) the results for three different tilt angles are shown. The solid lines represent the calculated positions according to Eq. (3).

In (b) the corresponding results for an in-plane magnetic field and a different sample are shown. Here, we also depict the amplitude of the observed resonance together with the theoretically expected one. As can be seen, the agreement between the simple model of two coupled harmonic oscillators and our experimental results is quite perfect. There is no fit parameter in the calculations, the sloshing mode  $\omega_0$  is simply taken from the growth parameters of our samples. Changing the carrier density does not change the extracted resonance position  $\omega_0$  significantly [13], indicating that Kohn's theorem is valid for our systems. To demonstrate the sensitivity of the above experiments we show in Fig. 3 typical spectra taken at a very small tilt angle and for different magnetic fields between  $B = 2.5$  T and  $B = 4.0$  T. The interaction between the sloshing mode and the CR manifests itself in a sharp dip in the envelope of the spectra in the vicinity of the

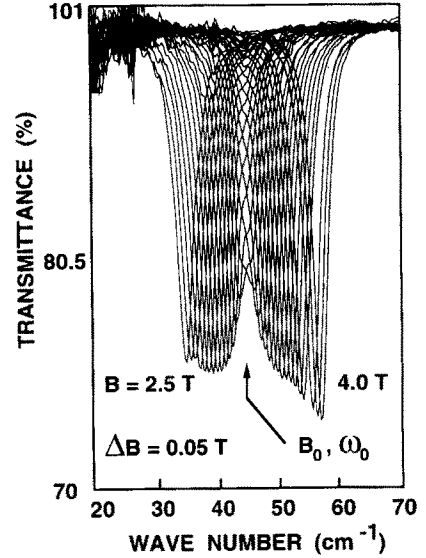


Fig. 3. Experimentally obtained spectra of the cyclotron resonance in a PQW in a tilted magnetic field. The tilt angle in this case is very small ( $\theta = 3^\circ$ ) such that a splitting of both lines according to Eq. (3) is not yet achieved. Nevertheless, a sharp dip in the envelope of the spectrum indicates the region of anticrossing between both lines and allows for an exact determination of the resonance condition.

degeneracy point, although a line splitting at this small angle is not yet resolved.

#### 4. Imperfect parabolic wells

So far, we have demonstrated the FIR response of “ideal” PQWs, where Kohn's theorem is valid. However, it is very interesting to investigate the effect of non-parabolic terms in the confining potential of the FIR spectrum. Here, too, PQWs seem to be a nearly perfect tool. Unlike the case of quantum wires or dots, the external confining potential can be tailored in a very precise and controlled way during the growth. Moreover, optical experiments on imperfect PQWs can yield information not only about the extent to which the confining potential deviates from perfect parabolicity, but also (for small deviations) about the forbidden excitations of an ideal system. Here, we present experimental results obtained in a structure where we intentionally

induced a certain degree of nonparabolicity to study its influence on the FIR spectrum [14]. The sample is a nominally 75 nm wide PQW with  $\Delta = 75$  meV, having vertical sidewalls which are 150 meV high. From the PQW curvature we expect the bare harmonic oscillator frequency to be  $\omega_0 \hat{=} 86$   $\text{cm}^{-1}$ . Apart from changing the carrier density in the well by application of a gate bias we can simultaneously change the shape of the confining potential in this special sample. At high well filling the additional vertical sidewalls violate parabolicity, whereas at very low filling the wavefunction is squeezed against the lower vertical sidewall. At intermediate fillings we expect the sample to behave like a “normal” PQW. An experimental spectrum, as obtained using the grating coupler technique [14], is shown in Fig. 4a. Here, we plot the relative change in transmission versus FIR frequency for different carrier densities in the well. As can be seen, the electron

system not only absorbs at the frequency of the bare potential, but side lines appear in the spectrum. Experiments in a tilted magnetic field confirm this observation. Here, we make use of the effect of a certain “contrast enhancement” in such measurements: Although the oscillator strengths of the additional lines may be quite small as compared to the main line, their existence can also lead to a resonant interaction between these modes and the cyclotron resonance. This is demonstrated in Fig. 4b, where we plot the extracted resonance positions from a tilted field experiment for this sample as a function of the magnetic field and for three different gate voltages. Most remarkable is the occurrence of additional lines and the completely changed character of the dispersion as compared to an “ideal” PQW especially for low well fillings.

Recently, Dempsey and Halperin [15] were able to perfectly describe our experimental re-

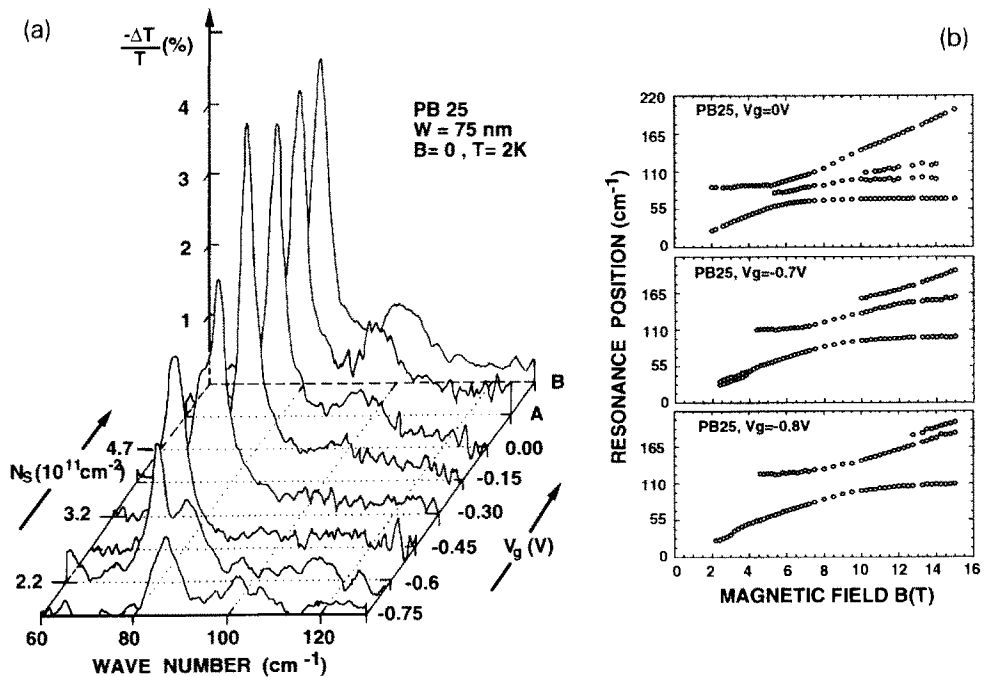


Fig. 4. (a) Grating-coupler-induced spectra for an imperfect PQW. The relative change in transmission is shown for different carrier densities  $N_s$ . In both limits of high and low well filling deviations from the harmonic oscillator picture are observed, manifesting themselves in the occurrence of additional lines [14]. (b) Experimentally obtained resonance positions from a tilted-field experiment on sample PB25 for different well fillings. With decreasing carrier density the spectra deviate more and more from the simple harmonic oscillator picture. Additional lines besides the CM modes appear and the whole spectrum is shifted towards higher energies, indicating a “stiffening” of the confining potential.

sults by using a self-consistent field approach in the local density approximation (LDA-SCF) and, for comparison, also in the random phase approximation (RPA). Since for our samples the shape of the confining potential is extremely well known, it allows for a completely satisfying explanation in terms of theoretical understanding. An important result is the strong mixing of the depolarization-shifted single-particle subband resonances that lead to the complicated spectrum as presented in Fig. 4. Our results together with the theoretical work thus can be regarded as a valuable approach towards the understanding of the FIR spectrum also of quantum wires and dots, where the confining potential is only in first-order parabolic, but not known a priori.

Experiments at finite wave vector are very illustrative in understanding the excitation spectrum of parabolically confined electron systems. Here, we use a grating coupler technique of periodicity  $a$  to couple also to intrasubband plasmon excitations. In a local and strictly two-dimensional treatment, where the wavelength of the

excitation is taken to be much larger than the thickness of the electron system, this dispersion of the intrasubband plasmon reads

$$\omega_p^2 = \frac{e^2 N_s q_x^n}{2\bar{\epsilon} m_p}, \quad \text{with} \quad q_x^n = n \frac{2\pi}{a}. \quad (4)$$

Here,  $N_s$  again denotes the areal carrier density,  $\bar{\epsilon}$  is an effective dielectric function including screening, and  $m_p$  is a plasmon effective mass. It is important that in the near field of the grating,  $z$ -components of the electric field are induced which can be used to excite the intersubband like resonances as discussed in the previous section (cf. Fig. 4a). In the limit of small  $q$  we expect Eq. (4) still to be reasonably valid, even though we are not dealing with a strictly 2D system. For reasonable carrier densities as present in our PQW, and for a wave vector of the order of  $2\pi/1 \mu\text{m}$ , the energies of the intrasubband plasmon  $\omega_p$  are of the same order as  $\omega_0$ . Thus we are able to systematically study the mutual interaction between both modes which is not that easily

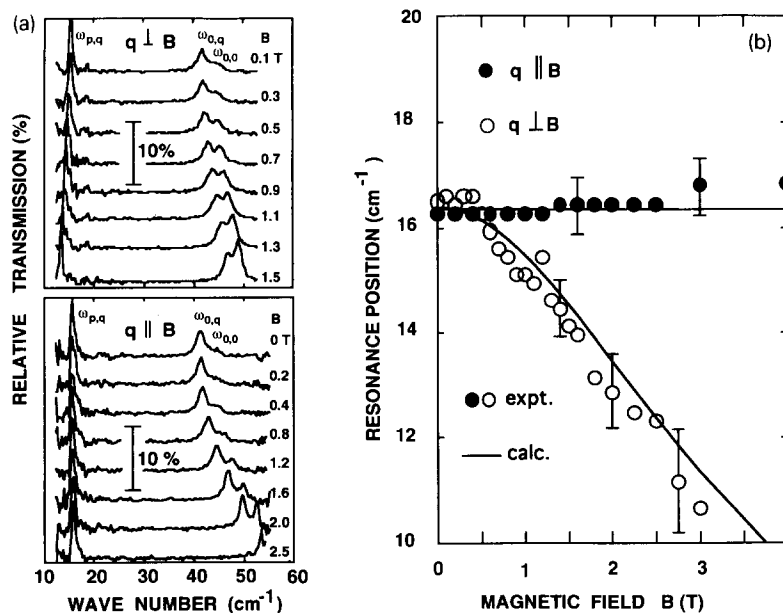


Fig. 5. Plasmon excitations of a PQW subjected to an in-plane magnetic field. The magnetic field induced anisotropy in the subband structure is clearly seen for the intrasubband plasmon resonance at around  $15 \text{ cm}^{-1}$ . For  $q \perp B$  the intra subband plasmon exhibits a negative magnetic field dispersion as it is typical for edge-type plasmons. No such signature is observed for  $q \parallel B$ . The agreement between the simple model as described in the text and the experimental results is quite perfect [17].

achieved on a 2DES. We find that both modes strongly couple if more than one electric subband is occupied, and some asymmetry is induced in the confining potential [16]. Due to the limited space in this report I have to refer the reader to the original paper addressing this mode-coupling phenomenon. There is, however, another very interesting feature about the intrasubband plasmon in a wide PQW: As we have seen before, an in-plane magnetic field hybridizes the cyclotron motion and the sloshing mode of a PQW similar to the magnetic field dispersion of the 1D inter-subband resonance or to the “upper” mode of the characteristic spectrum of a quantum dot. On the other hand, it turns out that the presence of an in-plane magnetic field induces an anisotropy in the subband dispersion. Taking the in-plane magnetic field to be directed along the  $y$ -direction, this dispersion then reads

$$E = \hbar\Omega(n + 1/2) + \frac{\hbar^2 k_x^2}{2m^*} \frac{\omega_{0,q}^2}{\Omega^2} + \frac{\hbar^2 k_y^2}{2m^*}, \quad (5)$$

where  $\Omega^2 = \omega_{0,q}^2 + \omega_{2c}^2$  denotes the effective hybrid mode at finite  $q$ . The free motion in the plane of the electron system is represented by the quasi-momenta  $k_x$  and  $k_y$ . The interesting fact is the occurrence of an anisotropic band structure with respect to the direction of the magnetic field. It is worth mentioning that Eq. (5) has exactly the same form for a Q1DES in the parabolic approximation if one replaces the term containing  $k_y$  by the 2D subband energy of the “starting material” Q2DES. The term containing  $k_x$  is then related to so-called one-dimensional plasmons propagating along the wire [5]. Eq. (5) can also be regarded as to describe a renormalization of the effective mass  $m^*$  with respect of the magnetic field direction. In terms of a collective excitation at finite  $q$ , this leads to a strongly anisotropic magnetic field dispersion, given by

$$\omega_{p,q}^2 = (\omega_{p,\perp}) = \omega_p^2 \left( 1 + \frac{\omega_c^2}{\omega_{0,q}^2} \right)^{-1}; \quad \omega_{p,q}^2 (q_{\parallel}) = \omega_p^2. \quad (6)$$

Here, the subscripts of  $q$  have to be taken with respect to the direction of the magnetic field  $B$ . The result of an experiment [17] where we probe this dispersion by a surface plasmon of the type given by Eq. (5) is shown in Fig. 5. In Fig. 5a we depict the experimental spectra for both magnetic field orientations. In all cases we observe three distinct lines with characteristic  $B$ -dispersion. For  $q \perp B$  the low energy line, which we identify with the intrasubband plasmon exhibits a negative dispersion which is characteristic for an edge-type plasmon mode. The lines with positive  $B$ -dispersion are identified as the sloshing mode at  $q = 0$  and at somewhat lower energy the one at finite  $q$  [17]. For  $q \parallel B$ , however, the intrasubband plasmon shows no magnetic field dependence as predicted by Eq. (7). In Fig. 5b we show the extracted resonance position for this plasmon and both magnetic field orientations. Again, there is quite perfect agreement with the calculation according to Eq. (7) as depicted by the solid lines.

As a final example, I would like to present

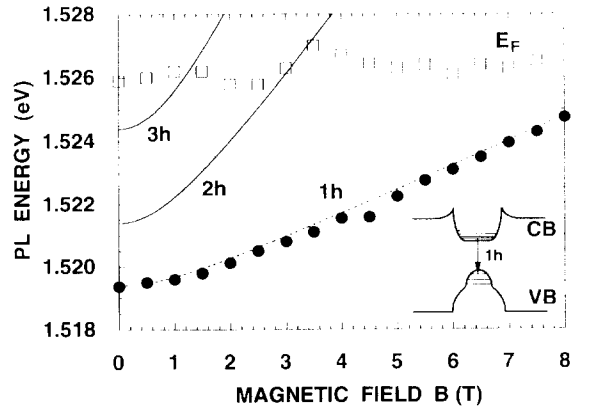


Fig. 6. Magneto-luminescence on a PQW subjected to an in-plane field at an excitation energy of 2.412 eV. In this experiment the single particle subband spectrum is probed by radiative recombination of photoexcited carriers in the quantum well. Strong confinement of the holes also leads to a Fermi edge singularity that allows for a determination of the Fermi level in the system. For symmetry reasons, only the transition 1h is observed. The lines depict the expected dispersion of the magneto-electric hybrid subbands that become depopulated at magnetic fields where the Fermi level exhibits characteristic kinks [courtesy of Ch. Peters, to be published].

some experimental results demonstrating that the single particle spectrum of a PQW is accessible with optical methods. Similar to the work of Plaut et al. [18], we investigated the magneto-photoluminescence (PL) of our samples in the above 1D geometry, i.e., the magnetic field directed along the plane of the electron system. Then, the magneto-electric hybrid bandstructure is identical to the one observed in quantum wires in a perpendicular magnetic field. Plaut et al. observe a PL signal that is attributed to the radiative recombination of such 1D-confined photoexcited electrons with holes that are provided by a p-type  $\delta$ -layer in close vicinity of the electron system. For a PQW, however, because of the graded alloy, both the conduction as well as the valence band of a PQW are parabolically shaped. This offers the advantage that there is also strong confinement for photoexcited holes, leading to a so-called “Fermi edge singularity” in the PL spectra allowing for a determination of the Fermi energy as a function of the applied magnetic field. In Fig. 6 we depict the result of such an experiment. Clearly the magnetic field dispersion of the lowest hybrid subband as well as the depopulation of the higher subbands is observed, as indicated by the oscillations of the Fermi level as a function of the magnetic field.

## 5. Acknowledgements

I would like to gratefully acknowledge a very fruitful collaboration with many colleagues as cited in the references and thank both the Deutsche Forschungsgemeinschaft and the Volkswagen Stiftung for financial support during the progress of this work.

## 6. References

- [1] For an excellent review on the electronic properties of low-dimensional systems, see, e.g., T. Ando, A.B. Fowler and F. Stern, *Rev. Mod. Phys.* 54 (1982) 437.
- [2] See, e.g., D. Heitmann, *Two-Dimensional Systems: Physics and New Devices*, Eds. G. Bauer, F. Kuchar and H. Heinrich (Springer, Berlin, 1986) p. 285.
- [3] For a recent review, see, e.g., W. Hansen, U. Merkt and J.P. Kotthaus, in: *Semiconductors and Semimetals*, Vol. 35, Eds. R.K. Williardson, A.C. Beer and E.R. Weber (Academic Press, San Diego, 1992) p. 279.
- [4] W. Hansen, M. Horst, J.P. Kotthaus, U. Merkt, Ch. Sikorski and K. Ploog, *Phys. Rev. Lett.* 58 (1987) 2586.
- [5] T. Demel, D. Heitmann, P. Grambow and K. Ploog, *Phys. Rev. Lett.* 64 (1990) 788.
- [6] Ch. Sikorski and U. Merkt, *Phys. Rev. Lett.* 62 (1989) 2164.
- [7] K. Karrai, H.D. Drew, H.W. Lee and M. Shayegan, *Phys. Rev. B* 39 (1989) 1426.
- [8] K. Karrai, X. Ying, H.D. Drew and M. Shayegan, *Phys. Rev. B* 40 (1989) 12020.
- [9] E.G. Gwinn, R.M. Westervelt, P.F. Hopkins, A.J. Rimberg, M. Sundaram and A.C. Gossard, *Phys. Rev. B* 39 (1989) 6260.
- [10] K. Ensslin, A. Wixforth, M. Sundaram, P.F. Hopkins, J.H. English and A.C. Gossard, *Phys. Rev. B* 47 (1993) 1366.
- [11] K. Karrai, X. Ying, H.D. Drew, M. Santos, M. Shayegan, S.R.E. Yang and A.H. MacDonald, *Phys. Rev. Lett.* 67 (1991) 3428.
- [12] L. Brey, N.F. Johnson and B.I. Halperin, *Phys. Rev. B* 40 (1989) 647.
- [13] A. Wixforth, M. Sundaram, K. Ensslin, J.H. English and A.C. Gossard, *Surf. Sci.* 267 (1992) 523.
- [14] A. Wixforth, M. Sundaram, K. Ensslin, J.H. English and A.C. Gossard, *Phys. Rev. B* 43 (1991) 10000.
- [15] J. Dempsey and B.I. Halperin, *Phys. Rev. B* 45 (1992) 3902.
- [16] M. Kaloudis, K. Ensslin, A. Wixforth, M. Sundaram, J.H. English and A.C. Gossard, *Phys. Rev. B* 46 (1992) 12469.
- [17] A. Wixforth, M. Kaloudis, M. Sundaram and A.C. Gossard, *Solid State Commun.* 84 (1992) 861.
- [18] A.S. Plaut, H. Lage, P. Grambow, D. Heitmann, K. von Klitzing and K. Ploog, *Phys. Rev. Lett.* 67 (1991) 1642.